BJBMB

Biobacta Journal of Biochemistry and Molecular Biology

https://bjbmb.org

SPBH

Original article

Gold Nanoparticles Cytotoxicity against Esophageal Carcinoma Cells: An In Vitro Study Using Glutathione-Modified Nanoparticles

Mustafa Basim Mohammed Al Tameemi[1], Mohammed M Abdulkadhm[2]

[1]Department of Medical Biotechnology, College of Biotechnology, University of Al-Qadisiyah, Iraq.

[2]University of Al-Qadisiyah, Al-Qadisiyah, Iraq.

DOI: https://doi.org/10.71428/BJBMB.2026.0209

Abstract

Background: Esophageal carcinoma remains an aggressive malignancy with poor prognosis and limited treatment options. Nanotechnology has introduced opportunities in cancer therapy, using gold nanoparticles (GNPs) due to their biocompatibility and tunable properties. **Objective:** This study evaluates the cytotoxic effects of glutathione-modified GNPs on the SK-GT-4 esophageal carcinoma cell line. **Methods:** GNPs were synthesized using a chemical reduction method and functionalized with glutathione (GSH) for stability. SK-GT-4 cells were cultured under standard conditions and exposed to GNP concentrations of 10–100 µg/mL. Cytotoxicity was evaluated via MTT assay, and morphological changes were observed using phase-contrast microscopy. Cell cycle and apoptosis were measured by flow cytometry. Expression patterns of p53, caspase 3, and caspase 8 were studied by quantitative real-time PCR (qPCR). Data were analyzed using unpaired t-tests ($p < 0.05$). **Results:** FTIR analysis confirmed glutathione conjugation to the GNPs, which induced a significant dose-dependent cytotoxic effect on SK-GT-4 cells, with an IC_{50} of approximately 8.694 µg/mL. Morphological changes consistent with apoptosis, including rounding and detachment, were observed. At 2MIC, the proportion of cells arrested in the Gap2/mitosis (G2/M) phase increased from 10% (control) to 18.04% ($p < 0.05$). Early apoptotic cells increased from 5% (control) to 18.11% at 2MIC. p53 and caspase 3 were elevated, while caspase 8 was downregulated, indicating that GNPs modify the regulation of apoptotic genes in SK-GT-4 cells.

Conclusion: Glutathione-modified GNPs exhibit significant cytotoxic potential against esophageal carcinoma cells, suggesting their promise as nanotherapeutic agents. Further mechanistic and in vivo evaluations are necessary to assess their clinical application.

Keywords: Gold nanoparticles, Glutathione, Esophageal carcinoma, SK-GT-4, Cytotoxicity, Apoptosis.

Introduction:

Esophageal cancer ranks as the eleventh most diagnosed cancer worldwide. It's also the seventh leading cause of cancer-related fatalities. The weight of this aggressive disease falls heavily on developing regions, which bear about 80% of cases. Among those afflicted, approximately 70% are men. Interestingly, there's a striking threefold gap in incidence and mortality rates between the sexes [1]. Furthermore, esophageal cancer is more common among the elderly, and the risk of having it rises with age. It is anticipated that the cancer burden of esophageal cancer would gradually rise due to the expansion and aging of the world's population as well as the persistence of related risk factors. Furthermore, esophageal cancer frequently has a poor prognosis because of its high degree of aggressiveness. In most countries, the 5-year

Received: June 4, 2026. Accepted: August 10, 2026. Published: September 12, 2026

survival rate after diagnosis is quite low, ranging from about 10% to 30% [2]. The burden of esophageal cancer varies significantly among different countries and populations, which is related to the underlying risk factors for prevalence and the differences in the distribution of subtypes [3].

The 5-year survival rate following diagnosis is rather poor in the majority of countries, ranging from roughly 10% to 30% [2]. Due to variations in the distribution of subtypes and underlying risk factors for prevalence, the burden of esophageal cancer varies greatly between nations and people [3].

Because gold nanoparticles (AuNPs) can increase therapeutic efficacy and reduce adverse effects, they are being thoroughly studied for the treatment of esophageal cancer. They function as radiosensitizers, which exacerbate radiation-induced tumor damage, and as powerful agents in photothermal therapy, which turns light into heat to kill cancer cells. They also act as specific delivery systems for chemotherapeutic medications [4]. The majority of esophageal malignancies globally are esophageal squamous cell carcinomas (ESCCs), which have a dismal prognosis and growing resistance to standard therapies. Traditional treatment methods (radiation, chemotherapy, surgery, or a combination of these) have many drawbacks, including delayed diagnosis, 5-year survival rates below 20%, systemic toxicity of the drugs used, and the development of treatment resistance [5].

In light of these difficulties, nanotechnology has become a novel and potential treatment option in oncology in recent years [6]. Numerous pharmacological benefits are provided by nanoparticles (NPs), whether they are based on oxides, polymers, lipids, or metals (gold, silver, copper). Better solubility of active ingredients, targeted and regulated release, and, most importantly, greater permeability and retention (EPR effect) at the tumor level are among their benefits. This allows for the preferred targeting of cancer cells while minimizing exposure of healthy tissue [7].

Furthermore, certain NPs have inherent antitumor activity through the production of reactive oxygen species (ROS), modification of mitochondrial function, or induction of apoptosis, which makes them promising therapeutic agents [8]. In cancer, nanotechnology has become a game-changing instrument. Gold nanoparticles (GNPs) have exceptional biocompatibility, surface modifiability, easy production, and special optical qualities. Enhancing therapeutic potential, functionalization with glutathione (GSH) increases cellular absorption, decreases aggregation, and improves nanoparticle stability. Gold nanoparticles coated with the biodegradable tripeptide glutathione are known as glutathione-conjugated gold nanoparticles (GSH-AuNPs). This alteration greatly improves their colloidal stability, facilitates effective urine clearance, and offers a "stealth" action by lowering serum protein adsorption. They are ideal platforms for drug administration, targeted cancer therapy, and sensitive electrochemical sensing applications in biological contexts because of their surface functional groups (like carboxyls) and biocompatibility [9].

Glutathione (GSH) is a biodegradable polymer that has gained popularity recently. GSH-coated nanoparticles are made from this polymer. As a drug delivery vehicle, GSH-coated gold nanoparticles (GNPs) have demonstrated tremendous promise [10]. Among the several biodegradable polymers that are currently available, GSH is the most widely used due to its extensive clinical use, advantageous breakdown properties, and potential for long-term drug administration. Additionally, peptides have been employed as targets that can attach to a molecule on the nucleus' surface and pass through it [11].

GNPs have been shown to have anticancer effects in lung, colon, and breast malignancies in earlier research. Nevertheless, their effectiveness against esophageal adenocarcinoma—specifically, the SK-

GT-4 cell line generated from Barrett's epithelium—has not received much attention. Using flow cytometry and apoptotic investigations, this study seeks to assess the lethal impact of GSH-modified GNPs on this pertinent cancer model (SK-GT-4 cell line).

Materials and Methods

Synthesis of Glutathione-Modified GNPs:

About 10ml of Gold (III) chloride ($AuCl_3$; 0.025 M) was mixed with 80ml of glutathione (0.019M; pH 8) and mixed thoroughly. Sodium borohydride ($NaBH_4$, 2mg/mL) was added dropwise under stirring and allowed to react overnight. The colour change confirms the formation of GNPs. The contents were centrifuged at 10,000rpm for 20min and washed three times with deionized water. The pellet obtained after washing was dried at 75^0C in a hot air oven, and the resulting GNPs were stored at 4 °C for further use.

Cell Culture:

SK-GT-4 cells were cultured in minimal essential medium (MEM) supplemented with 10% FBS, 100 U/mL penicillin, and 100µg/mL of streptomycin. The cells were cultured at 37°C in 5% CO_2. Subculturing was done twice weekly at 70–80% confluence. SK-GT4 cells were kindly donated by First centre/ Cell technologies scientific veterinary laboratory and FI Centre for Nanosciences, Baghdad city, Iraq. Concentrations ranging from 10 to 100 µg/ml were employed for the different studies after GAuNPs were dissolved in PBS (pH 6.8) and ultrasonicated for five minutes.

Characterization of the GNPs:

After 30min, UV absorbance was recorded to assess the stability and identification of the GAuNPs. FTIR spectra were acquired using a Nicolet 5700 FTIR spectrometer. DLS and scanning electron microscopy (SEM) (FEI ESEM Quanta 200) were used to investigate the nanoparticles' morphology.

MTT Assay:

Cell dissociation solution (0.2% trypsin, 0.02% EDTA, and 0.05% glucose in PBS) was used to trypsinize the cells [12]. After centrifugation, a 96-well plate was seeded with around $5x10^4$ cells/well and incubated for 24 hours at 37°C (5% CO_2). The medium was disposed of after a 24hr incubation period at 37°C in a 5% CO_2 incubator, and the monolayer was rinsed with the medium once. On the partial monolayer in microtiter plates, approximately 100µl of different test concentrations (10, 25, 50, 75, and 100µg/ml) of NPs were applied. After that, the plates were incubated for 24 hrs at 37°C. Following incubation, each well received 100µl of MTT (5 mg/10 ml of MTT in PBS) after the test solutions in the wells were removed. The plates were incubated at 37°C for 4 hr. After removing the supernatant, 100µl of DMSO was added, and the plates were gently shaken to dissolve the formazan that had formed.

A Gennex (USA) microplate reader operating at 590nm was used to measure the absorbance. The concentration of the necessary NPs to inhibit cell growth by 50% (IC_{50}) values were produced from the dose-response curves for each cell line, and the percentage growth inhibition was computed using the following formula. % cell viability = **((**OD of Control – OD of sample)/OD of Control) x 100.

Cell Cycle study on SK-GT-4 cells: In a 6-well plate with 2ml of serum-free medium, roughly $1x10^5$ cells were seeded and grown for 24 hours. After that, cells were cultured for 24 hrs with varying concentrations of the samples [13]. After incubation, the cells were harvested by centrifuging at maximum speed at room temperature. The pellet obtained was washed and resuspended in 2ml of 1X PBS. The cells were further treated with 300µl of sheath fluid. The cells were later fixed by adding 1mL of chilled 70% ethanol. After that, the cells were kept overnight at 4°C, and following incubation, the cells were centrifuged for 5min at 2000rpm after fixation. The pellet was washed with ice-cold 1X PBS, and following a 15min dark incubation period, the cell

pellet was resuspended in 450µl of sheath fluid (0.05mg/ml PI and 0.05mg/ml RNaseA). FACS Caliber (BD Biosciences, San Jose, CA; flow cytometry) was used to calculate the proportion of cells in different cell cycle stages in compound-treated and untreated populations [14].

Apoptosis detection:

Cell culture medium was used to plate $1X10^6$ cells per well in a 6-well plate the day before to apoptosis induction. Following an 18-hour incubation period, the wells were examined for floating (dead) cells, which were then pipetted out and replaced with fresh culture medium to the initial volume [13]. About 40 and 80µg/ml of the sample were used to trigger apoptosis in treated cells, which were then incubated for a full day. The cells were harvested and centrifuged at maximum speed. The pellet was washed with ice-cold 1X PBS and resuspended with 1ml of 1X Binding Buffer. About 500µL of cell suspension was added with 10µL of PI and 5µL of Annexin V and incubated at room temperature in the dark for 15min. Following incubation, a flow cytometer equipped with FCS Express software (FACS Caliber, BD Biosciences, San Jose, CA) was used to analyze the cells within an hour.

Morphological Analysis:

Morphological changes were examined under an inverted phase-contrast microscope at 10×. Apoptotic features such as shrinkage, rounding, and detachment were recorded.

Gene regulation of caspase 3, caspase 8, and p53 gene members:

RNA isolation: SK-GT-4 cells were washed twice with PBS and to the adherent cells 2ml of TRIzol (per T25 flask) was added and transferred to the tube and vortexed. About 0.2ml of chloroform per 1ml of TRIzol was added and the resulting mixture was centrifuged at maximum speed for 15mins at 4^0C. The upper aqueous phase was collected into a new clean tube and added with 0.5ml of isopropanol and mixed gently. The RNA precipitate was centrifuged at maximum speed for 10 min at 4^0C. Supernatant was discarded, and the RNA pellet was washed by adding 1ml of 70% ethanol and then resuspended in 25µl of DEPC-treated water [15].

RT-PCR: RT PCR was carried out according to [16], but with slight modifications. Using applicable biosystems, a semi-quantitative reverse transcriptase polymerase chain reaction (RT-PCR) (RT-PCR-CFX96 Biorad, USA) was performed to ascertain the quantities of 18srRNA and gene members. As directed by the manufacturer, the PrimeScript RT reagent kit (TAKARA) with oligodT and random hexamer primers was used to create the cDNA from 2 µg of RNA. The cDNA was synthesized for 30min at 50^0C, inactivated for 5min at 85^0C, and then diluted to twice the volume (1:2). Relative expression of gene members was calculated using the $2^{-\Delta\Delta Ct}$ equation.

Table: List of primers used. [17].

Name		length	Tm	GC%	Sequence
p53	FW	21	58.6	55	TAACAGTTCCTGCATGGGCGGC
	RV	21	56.8	55	AGGACAGGCACAAACACGCACC
caspase 3	FW	19	56	50	CTG GTT TTC GGT GGG TGT G
	RV	20	58	50	ACG GCA GGC CTG AAT AAT GAA
caspase 8	FW	20	56.5	55	CTG GTC TGA AGG CTG GTT GT
	RV	20	56.5	55	CAG GCT CAG GAA CTT GAG GG
18srRNA	FW	20	60.3	55	GGAGTATGGTTGCAAAGCTGA
	RV	20	58.8	55	ATCTGTCAATCCTGTCCGTGT

Statistical Analysis: Data were expressed as mean ± SD from three independent experiments. Statistical significance was analyzed using unpaired t-tests (GraphPad Prism 6.0); $p < 0.05$ was considered significant.

Results:

Characterization of GNPs:

UV Spectroscopic analysis: From UV spectroscopy data, the GNPs synthesized were shown to have higher absorbance. GNPs are recognized for showing absorption peaks between 520 and 570nm, which validates the observed outcome of glutathione-coated NPs. The resulting GNPs were confirmed by SEM analysis to be spherical and uniformly distributed, with an average size of 58.6 nm and a size range of 30 to 110 nm (Figure 3). The morphological form of the GNPs was spherical and primarily face-centered. At 100,000 and 25,000 magnifications, SEM micrographs revealed that the generated nanoparticles are spherical in shape and have a smooth surface with little aggregation.

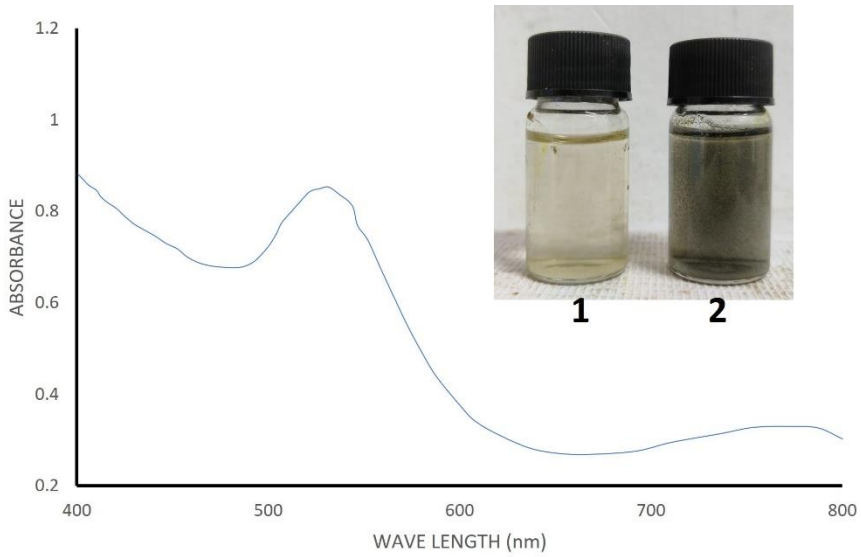

Figure 1: UV-Visible spectra of GNPs. UV spectra were recorded in the wavelength range of 400nm to 800nm. Colour change confirmation of NPs can be seen in the embedded image. **1:** AuCl3 solution; **2:** After GNP formation.

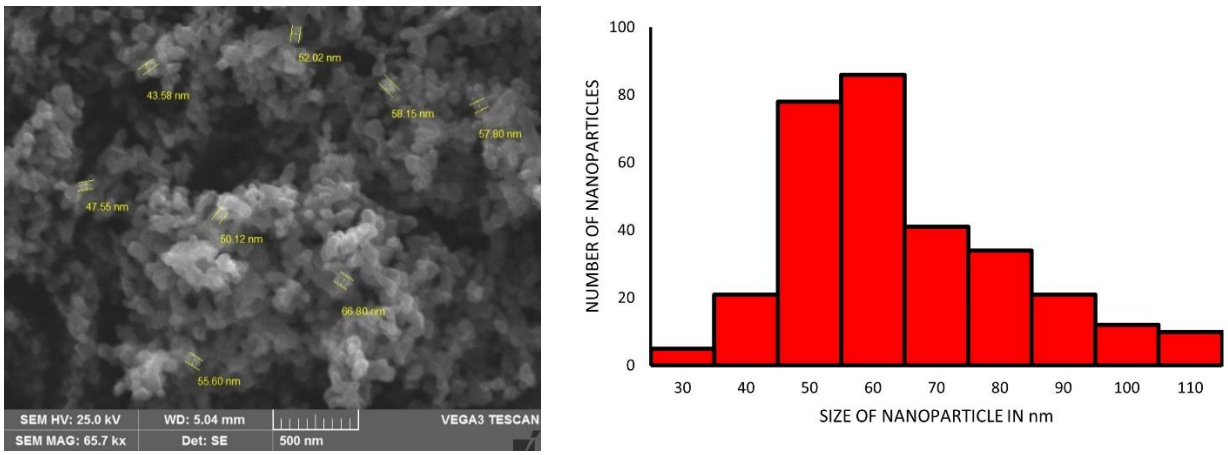

Figure 2: LEFT: SEM image of the GNPs synthesized. **RIGHT:** DLS analysis demonstrating the size distribution of the GNPs produced.

FTIR SPECTRA: The stretching vibrations of OH, H2O, and NH are responsible for the broad absorption band in the 3550–3240 cm^{-1} region. The v (SH) stretching mode, which shows up in the spectra for GNPs and indicates that Au NPs link to GSH via the sulphur atom, was the cause of the absorption band peaking at 2526cm^{-1} for GSH. The C=O stretching vibration of the glycine residue's –COOH group is responsible for the peak in GSH that was detected at 1650 cm^{-1}. The deprotonation of GSH's carbonyl group is indicated by this signal in GNPs [18]. The symmetric and asymmetric stretching modes of the COO- vibration, which were displaced to 1414 and 1144 cm^{-1}, respectively, in GNPs, are responsible for the peaks at 1315 and 1219 cm^{-1}, indicating the binding of GSH to Au NPs [18]. GSH adherence to the Au NPs is responsible for the new peaks at 1315 cm^{-1}. The coordination of GSH with Au NPs intensifies the C-S stretching vibration at 633 cm^{-1} [19]. In summary, modifications to the GNPs FTIR spectrum verify that GSH has effectively bound to Au NPs, resulting in the creation of GNPs.

Cell Viability and Cytotoxicity: The MTT assay demonstrated a **dose-dependent cytotoxic effect** of glutathione-modified gold nanoparticles on the SK-GT-4 esophageal carcinoma cell line. Treatment with increasing concentrations of GNPs (ranging from X to Y µg/mL) significantly reduced cell viability compared to untreated control cells (**$p < 0.05$**). The calculated **IC_{50} value** for GNPs on SK-GT-4 cells was approximately 8.694µg/mL, indicating potent antiproliferative activity (Figure 5). Morphological assessment under an inverted microscope revealed typical signs of cytotoxic damage in treated cells, such as cell shrinkage, rounding, detachment from the culture surface, and reduced confluency (Figure 6).

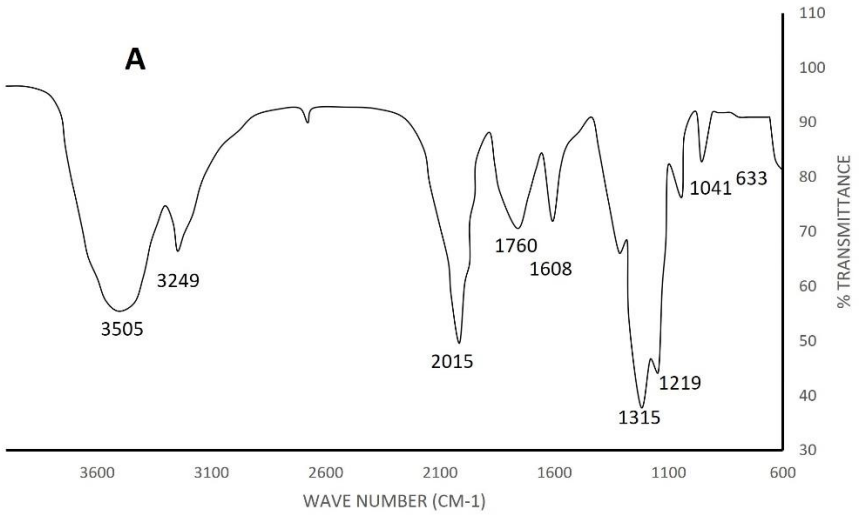

Figure 3: FTIR spectra of the $AuCl_3$ solution. Sharp bands of 3505, 3249, 2015, 1315, 1219cm^{-1} can be seen.

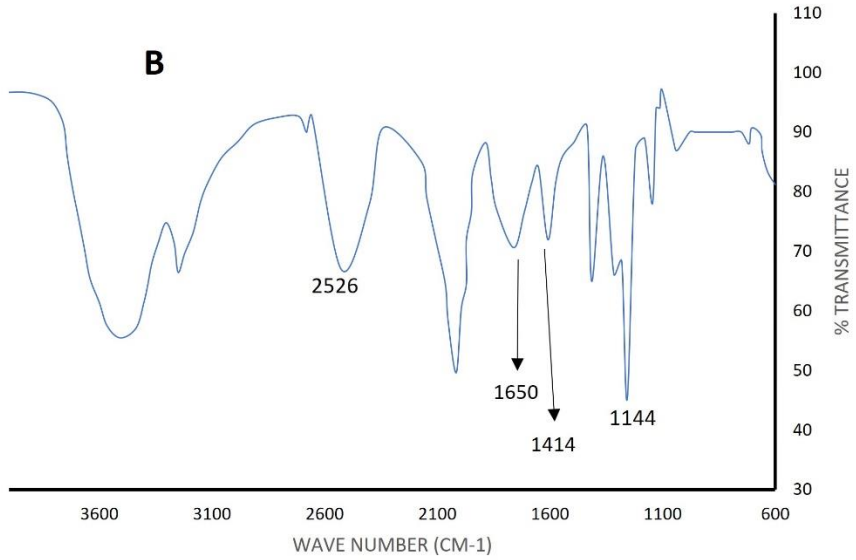

Figure 4: FTIR spectra of the synthesized GNPs. Sharp bands of 2526, 1650, 1414 and 1144cm^{-1} can be seen.

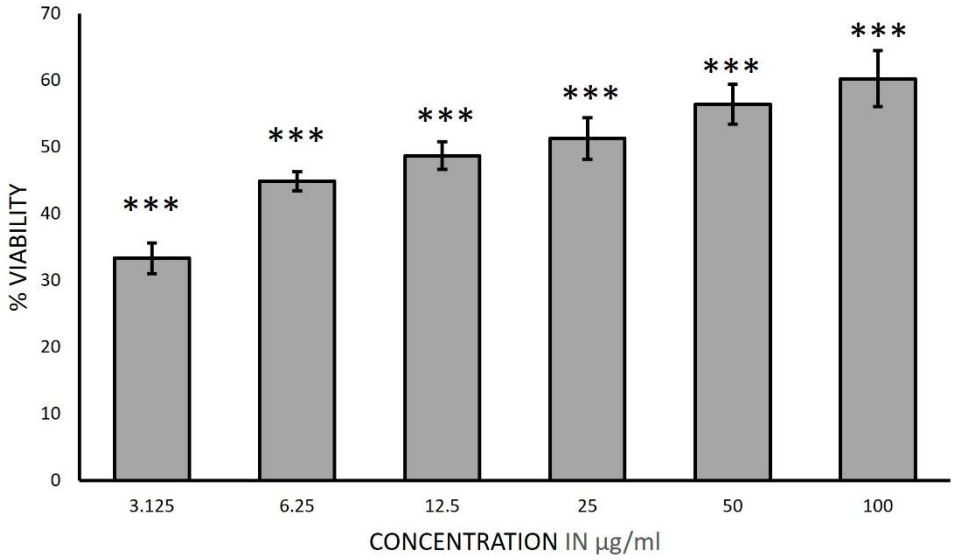

Figure 5: % CELL VIABILITY: sample (X) on SK-GT-4 cell line

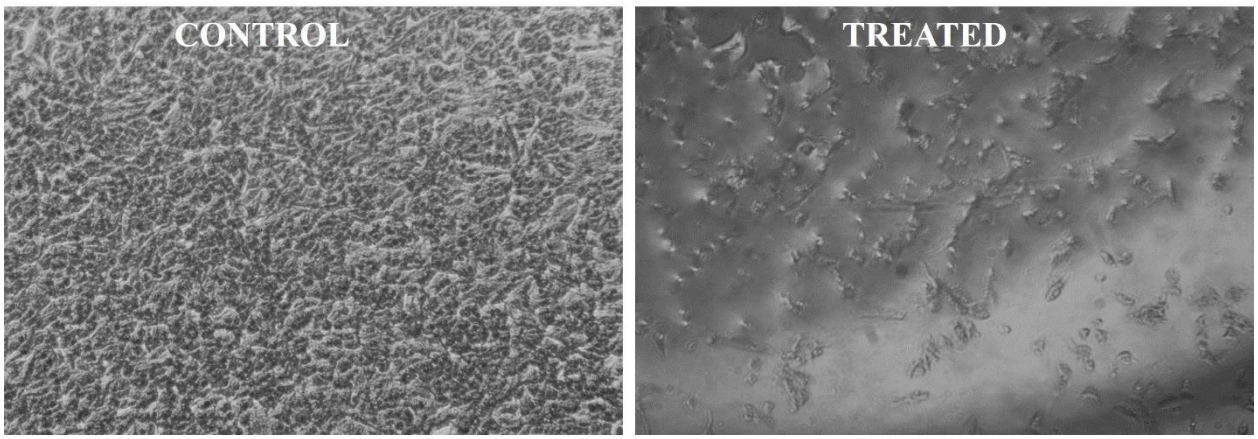

Figure 6: Morphological picture for oesophageal carcinoma cell line in vitro (a) Control cells (b) Cytotoxicity under an inverted microscope, 10x.

Cell cycle studies: As previously mentioned, the GNPs' IC50 value was 8.694µg/ml. The anticancer activity was planned at IC50 and 2IC50 values of 8 and 16µg/ml, respectively. The percentage of cells arrested in the Gap2/mitosis (G2/M) phase of the cell cycle rose from 10% (control) to 18.04% at the 2MIC concentration of GNPs when the concentration of GNPs increased from 8µg/ml to 16µg/ml. When compared to the positive control (colchicine) (24%), this is extremely significant (P<0.05). Compared to the positive control (Colchicine) (15.11%), approximately 6.14% of them are now arrested in the DNA synthesis (S) phase at this drug concentration (2MIC) (Figure 7). For the positive control (Colchicine), Sub-G0 was determined to be 2%, indicating that 2% of the cell population was in apoptosis. The cells were gated at 4% using the sample at 16 µg/ml of GNPs, which is highly significant (p<0.05).

Apoptosis detection using PI Annexin V-FITC staining: The results indicated that the viability percent reduced from 98% (control) to 62.12% at 2MIC, which is highly significant when compared to the positive control (Vinblastine) (53.03%) P<0.05. It was discovered that the number of early apoptotic cells had risen to 18.11% (2MIC) from 5% (control). A good proportion of cells (9.1%) were pushed into late apoptosis at 2MIC from 4.11% (control), compared to the positive control (15.13%).

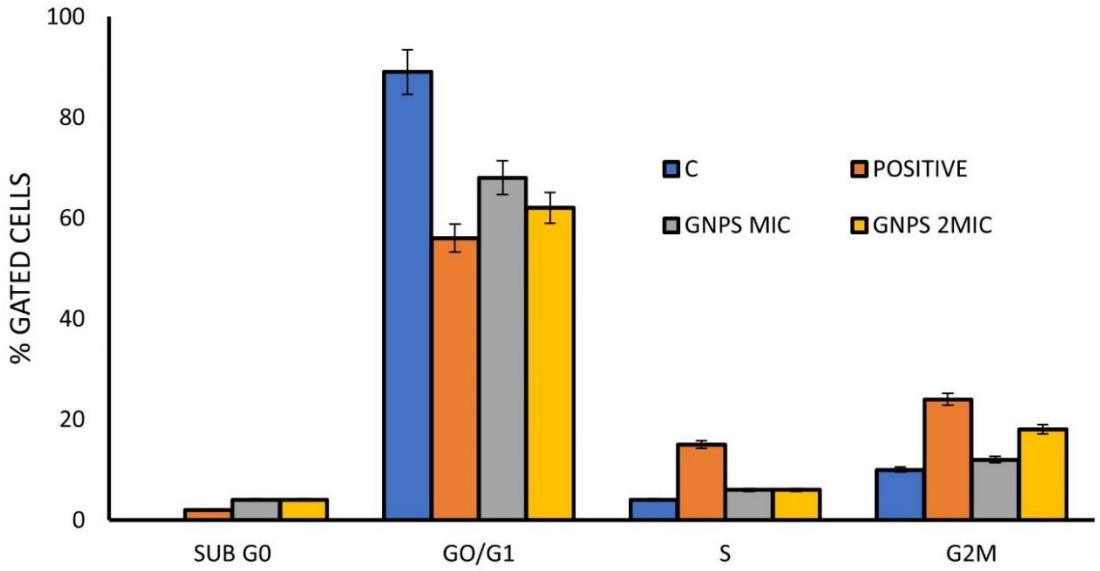

Figure 7: Graph showing the population histogram of the % gated cells in various cell cycle phases under the treatment of GNPs at MIC and 2MIC concentrations. The positive control was colchicine at MIC concentration.

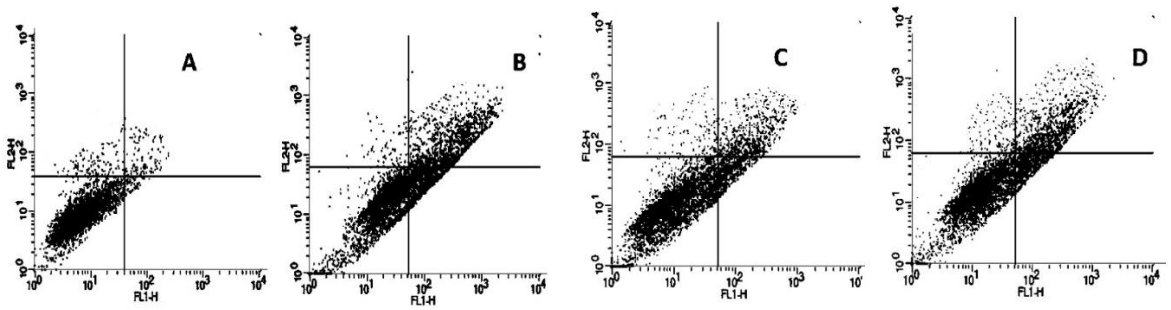

Figure 8: The figure shows the fluorescence scatter diagram of the cells. FSC-H Height and FL-2 Height represent Annexin-V-FITC and PI staining cells, respectively. A: control (untreated); B: Positive control; C: MIC**;** D: 2MIC.

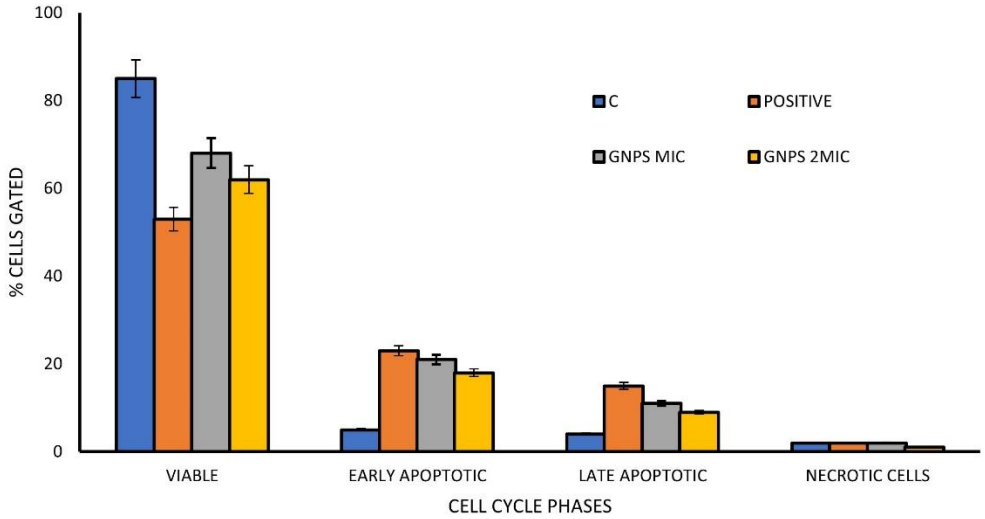

Figure 9: Figure showing the flow cytometry analysis of apoptosis detection in SK-GT-4 cells in various cell cycle phases with and without treatment of GNPs.

Gene regulation of caspase 3, caspase 8 and p53 gene members: When compared to the control (1 or 100%), the relative expression of p53 was found to be 1.4 times higher at MIC, while the positive control exhibited an elevation to 2.2 ($p<0.05$) (Figure 10). At 80µg/ml, the relative expression of caspase 3 was determined to be 0.18 times higher than the control (1 or 100%). There was a 0.23 ($p<0.05$) increase in the positive control (Figure 11). When compared to the control (1 or 100%), the relative expression of caspase 8 was found to be 0.27 times lower at 80µg/ml. A decrease to 0.33 ($p<0.05$) was observed in the positive control (Figure 12). Caspase 8 was shown to be downregulated, while p53 and caspase 3 were found to be upregulated. According to the research, GNPs alter how apoptotic genes are regulated in SK-GT-4 cells. The caspase 8 gene was shown to be downregulated, while the caspase 3 and p53 genes showed dose-dependent upregulation.

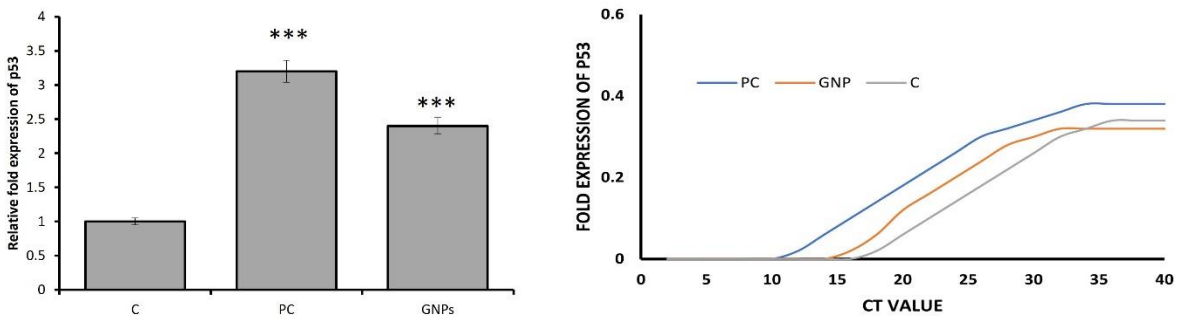

Figure 10: Figure showing the relative fold expression of the apoptotic gene p53 in SK-GT-4. C: control; PC: Positive control. Right: Ct values of the gene expression.

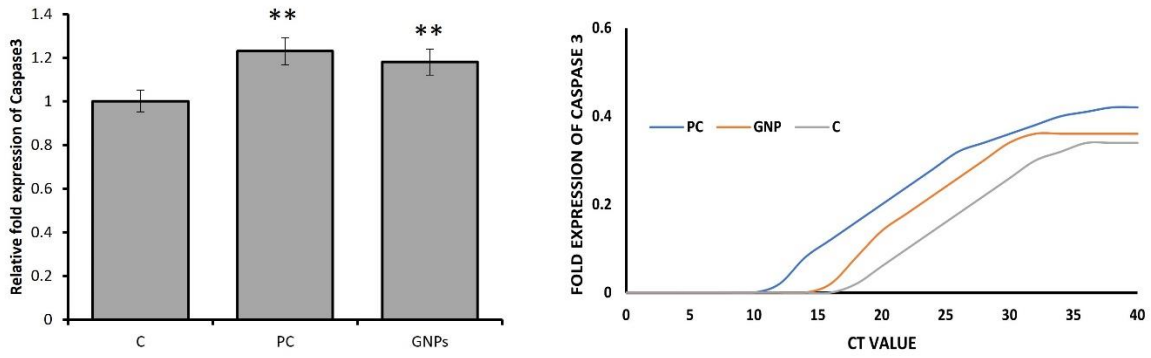

Figure 11: Figure showing the relative fold expression of apoptotic gene caspase 3 in SK-GT-4. C: control; PC: Positive control. Right: Ct values of the gene expression.

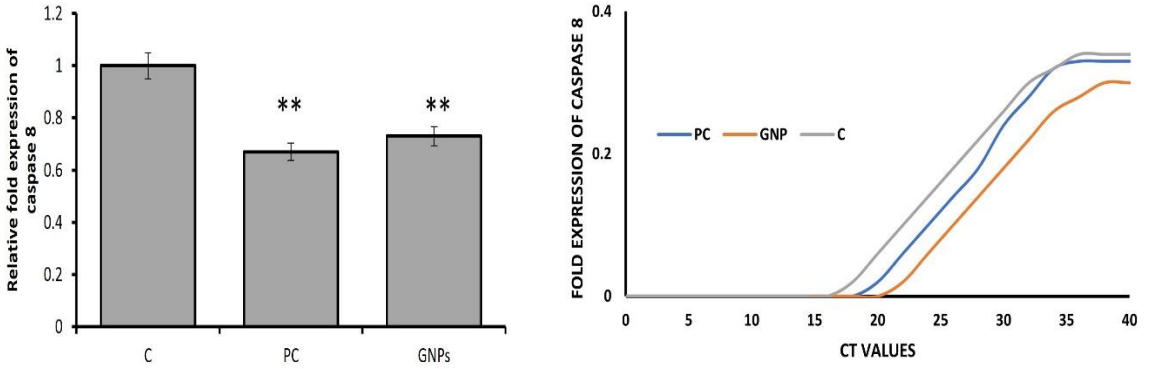

Figure 12: Figure showing the relative fold expression of apoptotic gene caspase 8 in SK-GT-4. C: control; PC: Positive control. Right: Ct values of the gene expression.

Discussion

One of the most deadly and aggressive cancers, esophageal cancer (EC) is responsible for a large percentage of cancer-related deaths globally [20]. Accurate pre-treatment staging and diagnostic methods have advanced significantly over the last three decades. The best treatment approaches are still up for debate; nevertheless, managing EC poses substantial therapeutic problems, especially when it comes to the function of radiation [21].

Due to their capacity to combine high stability with tumor-specific responsiveness, glutathione (GSH)-stabilized gold nanoparticles (Au-GSH NPs) have become a major development in nanomedicine for anticancer activity. Glutathione functions as a ligand and a capping agent, giving the nanoparticles special redox-sensitive characteristics that enable them to release therapeutic compounds or increase toxicity only in the tumor microenvironment while remaining stable in systemic circulation. To sum up, glutathione is an important stabilizer for gold nanoparticles because it offers a "smart" system that boosts drug delivery, decreases side effects through biocompatibility, and increases the death of cancer cells through both intrinsic qualities and targeted drug delivery.

Data from UV spectroscopy revealed that the produced GNPs had greater absorption. SEM analysis verified that the resultant GNPs were uniformly dispersed and spherical, with an average size of 58.6 nm and a size range of 30 to 110 nm (Figure 3). Similar confirmation was reported by [22], wherein they reported that gold nanoparticles less than 80nm were found to be spherical, and

particles above 100nm were icosahedral in shape. It was also discovered that colloidal gold nanoparticles (AuNPs), which were produced by reducing chloroauric acid utilizing silk sericin (SS) derived from Bombyx mori silk as a biotemplate, had a face-centered cubic (FCC) structure and a spherical form [23].

The MTT assay demonstrated a **dose-dependent cytotoxic effect** of glutathione-modified gold nanoparticles on the SK-GT-4 esophageal carcinoma cell line with an **IC_{50} value** of 8.694µg/mL, indicating potent antiproliferative activity (Figure 5). For feline fibrosarcoma cell lines with strong glycoprotein P activity, [24] found that doxorubicin coupled to glutathione-stabilized gold nanoparticles (Au-GSH-Dox) has greater cytotoxic effects than free doxorubicin.

[25] investigated the antiproliferative activity of gold nanoparticles (AuNPs) stabilized with reduced glutathione (GSH) and conjugated with doxorubicin (DOX), gemcitabine (GEM), or cytarabine (CTA) using the MTT assay in in vitro models such as human osteosarcoma cells (143B) and breast epithelial cells (MCF10A). They verified that the synthesized AuNPs have strong anticancer properties against the three cell lines. Using glutathione (GSH)-modified small-sized gold nanoparticles (AuNPs) in photothermal therapy (PTT), a study by [26] indicated the possible lethal effect on cancer cells rather than normal cells. Using both green and NIR laser irradiation, they demonstrated a significant harmful effect through GSH-AuNP buildup in cancer cells.

Our findings are consistent with studies such as [27], which reported that GNPs induced apoptosis in MCF-7 breast cancer cells. However, this study is among the few investigating GNP effects on esophageal adenocarcinoma using the SK-GT-4 model, contributing novel insights into this therapeutic strategy. Our work shows that GSH-modified GNPs have potent, dose-dependent cytotoxic effects on SK-GT-4 esophageal cancer cells. These effects are most likely mediated by oxidative stress, mitochondrial disruption, and apoptosis, similar to previous studies on GNPs in epithelial cancers. [28] examined the cytotoxic effects of conjugates of linalool–GNP (LG) and linalool–GNP–CALNN peptide (LGC) on ovarian cancer cells. The cytotoxicity test showed that LG and LGC were specifically harmful to cancer cells and caused apoptosis by triggering caspase-8, the p53 protein, and other apoptosis-related proteins. The real-time PCR gene expression tests for the target members also confirmed a similar pattern.

From our study Caspase 8 was shown to be downregulated, while p53 and caspase-3 were found to be upregulated. According to the research, GNPs alter how apoptotic genes are regulated in SK-GT-4 cells. The caspase 8 gene was shown to be downregulated, while the caspase 3 and p53 genes showed dose-dependent upregulation.

Research has shown that applying different nanoparticles (NPs) to cancer cell lines can either directly deliver the p53 gene or cause cellular stress that activates endogenous p53, hence upregulating the tumor suppressor protein p53. Increased apoptosis (programmed cell death) and decreased cancer cell growth are usually the results of this overexpression. The term "ROS" describes a class of chemically active O_2 derivatives, including hydroxyl radicals, peroxides, and superoxide anion, which have physiological relevance as signaling molecules to control basic life processes [29]. On the other hand, an excessive build-up of NP-induced ROS may lead to genetic instability and oxidative damage to DNA, which subsequently increases the occurrence and progression of tumors [30]. In this case, the p53 pathway will be activated to suppress tumor formation by either fixing the genotoxic injury or inducing apoptosis due to the genotoxic damage caused by the abnormal quantity of ROS.

According to research by [31], ZnO nanoparticles cause DNA damage, ROS production, and p53 activation in cancer cell lines such as HepG2

(hepatoblastoma) and A549 (lung cancer). Their investigation revealed an increase in the mRNA and protein levels of the apoptotic gene bax and the tumor suppressor gene p53. The Au-C225-p53 system, which uses gold nanoparticles and cetuximab (C225) to deliver p53 wild-type (WT) genes precisely to EGFR-overexpressing SKOV-3 ovarian cancer cells, is a highly effective EGFR-targeted nanotherapy, according to [32]. According to their method, p53 activity was restored, resulting in high-level expression of WT p53 protein, cell cycle arrest, substantial apoptosis, and tumor shrinkage in xenograft models. Research conducted by [33] also verified that treatment caused p53/p21 upregulation and DNA damage in IMR-90 (fibroblasts) and U251 (glioma) cells.

According to research by [34], different nanoparticle formulations can cause cancer cell lines to undergo apoptosis by upregulating and activating caspase-3, which is frequently brought on by the generation of reactive oxygen species (ROS) and mitochondrial damage. Specialized organic nanoparticles (nanocurcumin, PLGA-loaded agents) and metal-based nanoparticles (silver, zinc oxide, gold) are important examples. ZnO nanoparticles functionalized with juglone targeted SW480 colon cancer cells, exhibiting considerable cytotoxicity and inducing apoptosis, according to a study by [35]. G2/M cell cycle arrest and notable nuclear changes result from this nanocomposite's 5.01-fold and 2.75-fold increases in CASP8 and CASP9 expression, as well as a 6.18-fold rise in caspase-3 activity. Significant, dose-dependent, and time-dependent cytotoxic effect against human gastric adenocarcinoma (AGS) cells has also been demonstrated by green-synthesized gold nanoparticles using *Cardiospermum halicacabum* (CH-AuNP), with an increase in caspase-3 [36]. While many studies were in line with our quantitative PCR expression patterns, very few reports were done on SK-GT-4 cell lines, which reflects the strength of the paper. Further, protein expression analysis using blotting could be a limitation of our work.

Conclusion:

Glutathione-functionalized gold nanoparticles significantly reduced SK-GT-4 cell viability and induced morphological features of apoptosis. These results support their potential application as nanotherapeutic agents in esophageal cancer. Future research should involve detailed mechanistic analysis and in vivo validation. This study discovered a useful method for the manufacture of gold nanoparticles coated with glutathione. By using FTIR analyses, our findings verified the conjugation of glutathione with the gold NPs. When compared to the positive control alone, the synthesized GNPs were significantly more effective as antiproliferative agents against the SK-GT-4 cell line. Additionally, the outcomes showed that GNPs caused apoptosis in the treated cells and killed the cancer cells. The findings demonstrated that these substances might be employed as pharmaceuticals either on their own or in conjunction with other chemotherapeutics to treat various cancer cell types.

Conflict of interest: NIL

Funding: NIL

References

1. Xie SH, Fang R, Huang M, Dai J, Thrift AP, Anderson LA, et al. Association between levels of sex hormones and risk of esophageal adenocarcinoma and Barrett's esophagus. Clin Gastroenterol Hepatol. 2020;18:2701-2709.e3. doi:10.1016/j.cgh.2019.11.030.
2. Arnold M, Pandeya N, Byrnes G, Renehan PA, Stevens GA, Ezzati M, et al. Global burden of cancer attributable to high body-mass index in 2012: a population-based study. Lancet Oncol. 2015;16:36-46. doi:10.1016/S1470-2045(14)71123-4.
3. Conway E, Wu H, Tian L. Overview of risk factors for esophageal squamous cell carcinoma

in China. Cancers (Basel). 2023;15:5604. doi:10.3390/cancers15235604.

4. Nakhaeepour Z, Mashreghi M, Matin MM, NakhaeiPour A, Housaindokht MR. Multifunctional CuO nanoparticles with cytotoxic effects on KYSE30 esophageal cancer cells, antimicrobial and heavy metal sensing activities. Life Sci. 2019;234:116758. doi:10.1016/j.lfs.2019.116758.
5. Lagergren J, Smyth EC, Cunningham D, Lagergren P. Oesophageal cancer. Lancet. 2017;390(10110):2383-2396. doi:10.1016/S0140-6736(17)31462-9.
6. Ammar MM, Ali R, Abd Elaziz NA, Habib H, Abbas FM, Yassin MT, et al. Nanotechnology in oncology: advances in biosynthesis, drug delivery, and theranostics. Discov Oncol. 2025;16(1):1172. doi:10.1007/s12672-025-02664-3.
7. Yameny, A. A Comprehensive Review on Nanoparticles: Definition, Preparation, Characterization, Types, and Medical Applications. *Journal of Medical and Life Science*, 2024; 6(4): 663-672. doi: 10.21608/jmals.2024.419629
8. Siddiqi KS, Husen A. Green synthesis, characterization and uses of palladium/platinum nanoparticles. Nanoscale Res Lett. 2018;13:482.
9. Wang Y, Strohm EM, Sun Y, Wang Z, Zheng Y, Wang Z, et al. Biodegradable polymeric nanoparticles containing gold nanoparticles and paclitaxel for cancer imaging and drug delivery using photoacoustic methods. Biomed Opt Express. 2016;7(10):4125-4138. doi:10.1364/BOE.7.004125.
10. Sebastian S, Hoffmann MK, Howard D, Young C, Washington J, Unterweger H, et al. Kinetic effects of transferrin-conjugated gold nanoparticles on the antioxidant glutathione-thioredoxin pathway. Antioxidants (Basel). 2023;12(8):1617. doi:10.3390/antiox12081617.
11. Daraee H, Eatemadi A, Abbasi E, Fekri Aval S, Kouhi M, Akbarzadeh A. Application of gold nanoparticles in biomedical and drug delivery. Artif Cells Nanomed Biotechnol. 2016;44(1):410-422. doi:10.3109/21691401.2014.955107.
12. Viani Anggi, Masyita AA. Combination effects of Abelmoschus manihot (L.) Medik of N-hexane extracts and doxorubicin in breast cancer 4T1 cells line. Res J Pharm Technol. 2022;15(2):639-642. doi:10.52711/0974-360X.2022.00105.
13. Xia Q, Li X, Zhou H, Zheng L, Shi J. S100A11 protects against neuronal cell apoptosis induced by cerebral ischemia via inhibiting the nuclear translocation of annexin A1. Cell Death Dis. 2018;9(6):657. doi:10.1038/s41419-018-0686-7.
14. Jhaumeer Laulloo S, Bhowon MG, Soyfoo S, Chua LS. Nutritional and biological evaluation of leaves of Mangifera indica from Mauritius. J Chem. 2018;2018:6869294. doi:10.1155/2018/6869294.
15. Livak KJ, Schmittgen TD. Analysis of relative gene expression data using real-time quantitative PCR and the 2^-DeltaDeltaCT method. Methods. 2001;25(4):402-408. doi:10.1006/meth.2001.1262.
16. Malla Sudhakar, Venkata Raman B. Bactericidal and anti-biofilm activity of tannin fractions derived from Azadirachta against Streptococcus mutans. Asian J Appl Sci. 2020;13:132-143. doi:10.3923/ajaps.2020.132.143.
17. Al-Shammari AM, Abo-Altemen RA, Shawkat MS. Cyperus rotundus L. alkaloid extracts enhance oncolytic Newcastle disease virus against digestive system neoplasms. S Afr J Bot. 2021;143:266-273. doi:10.1016/j.sajb.2021.08.002.
18. Ou XX, Quan X, Chen S, Zhang FJ, Zhao YZ. Photocatalytic reaction by Fe(III)-citrate complex and its effect on the photodegradation of atrazine in aqueous solution. J Photochem Photobiol A Chem. 2008;197:382-388.
19. Basu S, Ghosh SK, Kundu S, Panigrahi S, Praharaj S, Pande S, et al. Biomolecule induced nanoparticle aggregation: effect of particle size

on interparticle coupling. J Colloid Interface Sci. 2007;313(2):724-734. doi:10.1016/j.jcis.2007.04.069.

20. van der Werf LR, Busweiler LAD, van Sandick JW, van Berge Henegouwen MI, Wijnhoven BPL; Dutch Upper GI Cancer Audit (DUCA) group. Reporting national outcomes after esophagectomy and gastrectomy according to the Esophageal Complications Consensus Group (ECCG). Ann Surg. 2020;271(6):1095-1101. doi:10.1097/SLA.0000000000003210.
21. Findlay M, Purvis M, Venman R, et al. Nutritional management of patients with esophageal cancer throughout the treatment trajectory: benchmarking against best practice. Support Care Cancer. 2020;28:5963-5971.
22. Battie Y, Izquierdo-Lorenzo I, Resano-Garcia A, En Naciri A, Akil S, Adam PM, et al. Determination of gold nanoparticle shape from absorption spectroscopy and ellipsometry. Appl Surf Sci. 2017;421(Pt B):301-309. doi:10.1016/j.apsusc.2016.12.167.
23. Nilogal, Asha, Sewar, Ranjana R, Harisha K, Shilpa ML, et al. Biosynthesis of spherical gold nanoparticles and their characterization. IOP Conf Ser Mater Sci Eng. 2019;577:012007. doi:10.1088/1757-899X/577/1/012007.
24. Zabielska-Koczywas K, Dolka I, Krol M, Zbikowski A, Lewandowski W, Mieczkowski J, et al. Doxorubicin conjugated to glutathione stabilized gold nanoparticles (Au-GSH-Dox) as an effective therapeutic agent for feline injection-site sarcomas-chick embryo chorioallantoic membrane study. Molecules. 2017;22(2):253. doi:10.3390/molecules22020253.
25. Steckiewicz KP, Barcinska E, Sobczak K, Tomczyk E, Wojcik M, Inkielewicz-Stepniak I. Assessment of anti-tumor potential and safety of application of glutathione stabilized gold nanoparticles conjugated with chemotherapeutics. Int J Med Sci. 2020;17(6):824-833. doi:10.7150/ijms.40827.
26. Al-Barram LFA. Laser enhancement of cancer cell destruction by photothermal therapy conjugated glutathione (GSH)-coated small-sized gold nanoparticles. Lasers Med Sci. 2021;36(2):325-337. doi:10.1007/s10103-020-03033-y.
27. Ali Z, Jabir M, Al-Shammari A. Gold nanoparticles inhibiting proliferation of human breast cancer cell line. Res J Biotechnol. 2019;14(S1):79-82.
28. Jabir M, Sahib UI, Taqi Z, Taha A, Sulaiman G, Albukhaty S, et al. Linalool-loaded glutathione-modified gold nanoparticles conjugated with CALNN peptide as apoptosis inducer and NF-kB translocation inhibitor in SKOV-3 cell line. Int J Nanomedicine. 2020;15:9025-9047. doi:10.2147/IJN.S276714.
29. Apel K, Hirt H. Reactive oxygen species: metabolism, oxidative stress, and signal transduction. Annu Rev Plant Biol. 2004;55:373-399.
30. Ng KW, Khoo SPK, Heng BC, Setyawati MI, Tan EC, Zhao X, et al. The role of the tumor suppressor p53 pathway in the cellular DNA damage response to zinc oxide nanoparticles. Biomaterials. 2011;32(32):8218-8225. doi:10.1016/j.biomaterials.2011.07.036.
31. Akhtar MJ, Ahamed M, Kumar S, Khan MM, Ahmad J, Alrokayan SA. Zinc oxide nanoparticles selectively induce apoptosis in human cancer cells through reactive oxygen species. Int J Nanomedicine. 2012;7:845-857. doi:10.2147/IJN.S29129.
32. Kotcherlakota R, Vydiam K, Jeyalakshmi Srinivasan D, Mukherjee S, Roy A, Kuncha M, et al. Restoration of p53 function in ovarian cancer mediated by gold nanoparticle-based EGFR targeted gene delivery system. ACS Biomater Sci Eng. 2019;5(7):3631-3644. doi:10.1021/acsbiomaterials.9b00006.
33. Mohamed HRH, Borai ME, Mosaad S, et al. Bioactive glass nanoparticles induce intrinsic p53-dependent apoptosis and promote genomic

instability via ROS overproduction and mitochondrial depolarization in triple-negative breast cancer cells. Sci Rep. 2026;16:809. doi:10.1038/s41598-025-32827-9.

34. Moawad M, Nasr GM, Osman AS, Shaker ES. Curcumin nanocapsules effect in apoptotic processes, gene expression, and cell cycle on Hep-G2 cell lines. Int J Immunopathol Pharmacol. 2023;37:3946320231176396. doi:10.1177/03946320231176396.
35. Safa A, Shafiei M, Sangari AN, et al. Targeted anticancer effects of Juglone-ZnO nanoparticles via cell cycle arrest and caspase-mediated apoptosis in colon cancer cells. Sci Rep. 2026;16:1513. doi:10.1038/s41598-025-31183-y.
36. Li C, Wang Y, Zhang H, Li M, Zhu Z, Xue Y. An investigation on the cytotoxicity and caspase-mediated apoptotic effect of biologically synthesized gold nanoparticles using Cardiospermum halicacabum on AGS gastric carcinoma cells. Int J Nanomedicine. 2019;14:951-962. doi:10.2147/IJN.S193064.